Event-based Single Molecule Localization Microscopy ($eventSMLM$) for High Spatio-Temporal Super-resolution Imaging

Jigmi Basumatary[1], Aravinth S[1], Neeraj Pant [1], Vignesh Ramanathan[2], Chetan Singh Thakur[2] and Partha Pratim Mondal [13*]
[1] *Mondal Lab, Department of Instrumentation and Applied Physics, Indian Institute of Science, Bangalore 560012, INDIA*
[2] *Department of Electronics System Engineering, Indian Institute of Science, Bangalore 560012, INDIA*
[3] *Centre for Cryogenic Technology, Indian Institute of Science, Bangalore 560012, INDIA*
(Dated: December 30, 2023)

Photon emission by single molecules is a random event that has a well-defined distribution. This calls for event-based detection in single-molecule localization microscopy. The detector has the advantage of providing the arrival time of photons and their distribution (emission characteristics) within a single blinking period (typically, $\sim 30\ ms$) of a single molecule. This information can be used to better localize single molecules within a user-defined collection time (shorter than average blinking time) of the event detector. The events collected over every short interval of time ($\sim 3\ ms$) give rise to several independent photon distributions (PSFs) of single molecules in the event camera. The experiment showed that single molecules intermittently emit photons. So, capturing events over a shorter period than the entire blinking period gives rise to several realizations of single-molecule PSFs. Specifically, this translates to a sparse collection of active pixels per frame on the detector chip (image plane). Ideally, multiple realizations of single-molecule PSF give several position estimates of the single-molecules, leading to multiple PSF centroids. Fitting these centroid points by a circle gives an approximate position (circle center) and geometric localization precision (circle area) of a single molecule. Since the single-molecule estimate (position and localization precision) is directly driven by the photon detection events and the recorded PSF, the estimated value is purely experimental rather than theoretical (Thomson's formula). Moreover, this eliminates the need for noise calculation and background estimation. The method is tested on three different test samples (1) Scattered Cy3 dye molecules on a coverslip, (2) Mitochondrial network in a cell, and (3) Dendra2HA transfected NIH3T3 cells (Influenza-A model). A super-resolution map is constructed and analyzed based on the detection of events / photons. Experimental results on transfected NIH3T3 cells show a localization precision of $\sim 10\ nm$, which is ~ 3.5 fold better than standard SMLM. Results reveal a spatio-temporal resolution ($l_p \times t$) of $122.5p$ (where, $p = 10^{-12}\ meter.second$) (measured in terms of localization precision). Cluster analysis of HA molecules shows $> 81\%$ colocalization with standard SMLM, indicating the consistency of the proposed $eventSMLM$ technique. Moreover, single-molecule imaging on live cells reveals the temporal dynamics (migration, association, and dissociation) of HA clusters for the first time over a period of 60 minutes. With the availability of event-based detection and high temporal resolution, we envision the emergence of a new kind of microscopy capable of high spatio-temporal super-resolution microscopy (in the range $\sim 1p = 10^{-12}\ meter.sec$).

I. INTRODUCTION

With the arrival of super-resolution microscopy, it is now possible to unveil the nanoscopic world of single molecules and their interaction in a cellular system. The techniques that largely facilitate super-resolution are either based on structured illumination or stimulated emission depletion (STED) or single molecule blinking (such as PALM, fPALM, STORM). These techniques have advanced so much that they are able to resolve features down to a few tens of nanometers. Needless to say, these techniques hold the potential to reveal biological processes in their natural environment.

Early 1990s saw the emergence of a new concept (called STED) that for the first time demonstrated the capability to surpass the diffraction limit [7] [1] [8]. It wasn't until early 2000s that the first far-field super-resolution technique is fully established [8]. Then the year 2005-2006 saw the emergence two different techniques (structured illumination and single molecule localization microscopy) that showed resolution far below the classical diffraction limit [9] [3] [2] [4]. This established the fact that it is possible to surpass the diffraction limit that was once thought impossible. Subsequent years saw the success of super-resolution technique and emergence of a family of variants. Most of these variants were inspired by applications in diverse disciplines ranging from biological to physical sciences. This include the development of STED [1] followed by stochastic optical reconstruction microscopy(STORM)[2], fluorescence photoactivated localization microscopy (f/PALM)[3][4] and DNApoint accumulation in nanoscale topography (PAINT)[5]. While STED is purely a RESOLFT based technique, PALM / fPALM / STORM are truly single molecule based techniques collectively known as Single Molecule Localization Microscopy (SMLM) [6]. Since the introduction of SMLM techniques, several variants are proposed to improve spatial resolution [10][11] [12][14][38][15]. Some of the key variants have revealed properties of single molecules such as, quantitative study of emitter orientation[23], multicolor imaging [29][30], molecule lifetime[26][27][28], single molecule tracking [34] and even information related to local neighborhood in a cellular system [24][25].

With the emergence of new applications, the need for better spatio-temporal resolution has increased. This calls for better localization precision and high temporal resolution. To overcome these two key obstacles, we propose event based detection of single molecules, practically realized by event detector/camera. These specialized detectors are different from sCMOS / EMCCD in the sense they are based on differential intensity, which means that event camera is sensitive to pixel-level brightness / intensity changes (ΔI) instead of intensity (I). They offer many advantages over traditional detectors (CCD EMCCD sCMOS) such as, no motion-blur and high temporal resolution in the order of few tens of microseconds. In standard detectors, each pixel synchronously integrates the incoming photon in a frame. The fixed frame of currently used detector technology limits the information of sporadic fluorescence emission of scholastically activated single molecules. Recently developed bio-inspired event-based detectors are demonstrated to promise the highest temporal resolution. This is due to the data-sensing architecture which is designed to monitor continuous changes in brightness(log intensity). When the changes in magnitude exceed the predefined threshold magnitude at a particular time, the camera sends an event having pixel location(x,y), time t, and the polarity p of the event. The polarity of an event is either positive(ON event) or negative(OFF event), corresponding to increased intensity or decreased intensity, respectively. Hence event camera output is a variable sequence of events(ON/OFF) with time and polarity. Asynchronously detected events are transferred to the periphery processing unit using a high readout bus called address-event representation (AER) readout bus[31]. More details and a survey on event cameras can be found in Ref. [32] [33].

The use of event camera in SMLM can be advantageous, primarily due to event-based detection and high temporal resolution. This facilitate determination of the position and localization of single molecules. The advantage of high temporal resolution and event sensitive detection allows recording of multiple realizations of the PSF within the blinking period. This has an advantage for detecting fortunate molecules (molecules that are bright). Ideally, centroids can be computed from individual PSFs and mean can be calculated along with its localization geometrically. This has the advantage of neglecting background noise, number of photons per molecule and noise pixelation factor as requited by standard SMLM. The technique is tested on multiple specimens such as, scattered Cy3 single molecules, and organelles (mitochondria) in a fixed cell. In a separate experiment, a Influenza (type A) disease model is considered

*Corresponding author: partha@iisc.ac.in

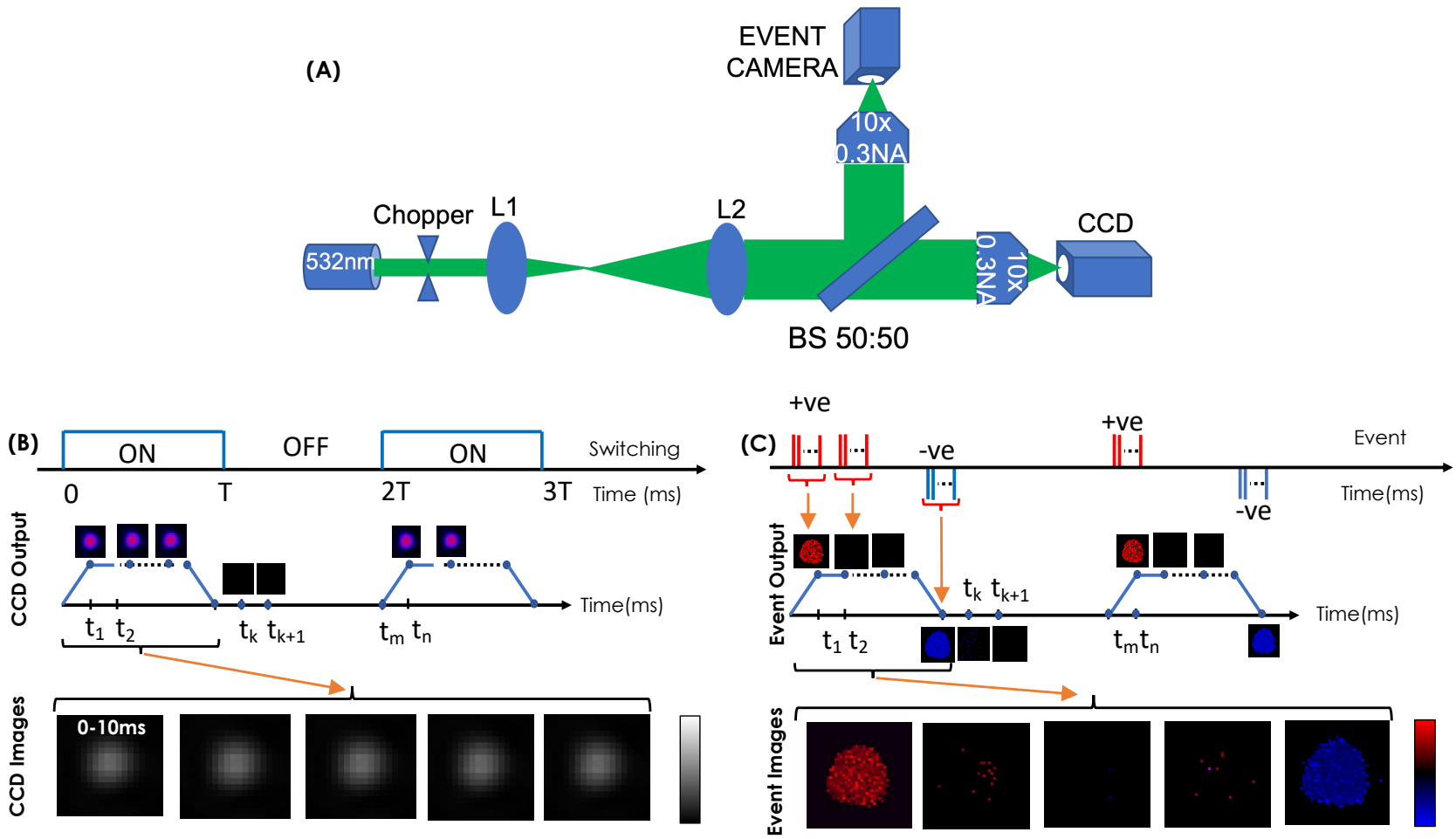

FIG. 1: A. Light switch-on / off event of 532nm continuous laser. The beam chopper is motorized in which driving voltage applied to it is controlled via a relay. Frequency of relay switching is programmed using Arduino. More details can be found in **Supplementary Note 2**. During the ON time, chopper is open, so laser light continuously falls on both the detector, whereas during OFF time, chopper stops the laser; as a result the laser does not enter into either detector. [B,C] Timing diagram of ON/OFF events and corresponding data recorded by CCD (EMCCD with zero gain) and event camera. The relay switching is providing a means to synchronize data from both the cameras. However this needs to be taken care of during processing the recordings. During the ON time of the chopper CCD detector shows the Gaussian profile of laser spot. However in case of event detector series of events are observed at a pixel(x, y), only whenever there is a rising edge (red spikes) or falling edge(blue spikes) of ON/OFF. This shown that event detector records only whenever there is change in intensity. Red spikes represents positive events corresponding to rising edge whereas blue spike represents negative events corresponding to falling edge. The event-based frames are recorded over the desired collection times (here, 10 ms) by collecting events (corresponding to pixel intensity).

where a key glycoprotein Hemaglutinin (HA) is monitored in live NIH3T3 cell determining HA cluster dynamics. The high spatio-temporal resolution of event camera is expected to substantially expand the reach of localization microscopy.

II. RESULTS

The *eventSMLM* technique involves event detection which essentially translates to the temporal detection of photons during detector ON time. However in traditional SMLM, the event corresponds to single molecule blinks and the detection by an intensity based CCD/EMCCD/sCMOS camera.

A. Event detection by Event Camera/Detector

The pixels in event camera are designed to record independently. Hence, the event detection can be understood at single pixel level. At time t_k and for a pixel position p_k, the change in intensity after time Δt_k is given by, $\Delta I(p_k, t_k) = I(p_k, t_k) - I(p_k, t_k - \Delta t_k))$. Using a first order approximation of Taylor series expansion, the change reduces to, $\Delta I(p_k, t_k) = \Delta t \frac{I(p_k, t_k)}{t}$. Noting that, the intensity is directly proportional to the number of photons i.e, $I \propto N$, and so the change in intensity is proportional to a corresponding change in the number of photons i.e, $\Delta I \propto \Delta N$. Accordingly, an event can be described as, $E_v = \frac{\Delta N}{\Delta t} = \frac{N(p_k, t_k)}{t}$. A detailed description for event detection can be found in **Supplementary 1**.

A simple optical setup for event detection is shown in Fig. 1A. The system is equipped with dual detectors i.e, standard EMCCD camera and an event camera. A 50:50 beam-splitter is introduced to split the expanded beam, and focussed on both the cameras. This is done to calibrate and understand the response of both the cameras under constant switch on/off illumination of laser beams. An electronic chopper is used to control ON / OFF state of the illumination light source (532 nm CW laser). Corresponding time diagram is shown in Fig. 1B. The CCD / EMCCD images are acquired during on/off state of the laser and the data is obtained at a time interval of 50 ms $(0-T)$ as shown in Fig. 1B. Positive and negative events corresponding to positive and negative change in intensity are also indicated along with the images captured by event camera in Fig. 1C. It is quite evident that event camera records non-zero images only during the rise and fall time. This clearly indicate the distinct characteristics of a EMCCD and event detector.

To decipher and characterise emission from a single molecule, we used event camera to capture data of Cy3 molecules at a sampling rates of 333 Hz (time-period, $\tau = 3ms$), 100 Hz ($\tau = 10ms$) and 33 Hz ($\tau = 30ms$). Fig. 2A shows the optical setup for simultaneous detection of single molecules in both the detectors (EMCCD and Event cameras) along with the PSF distribution and the corresponding geometric localization precision (see, **Supplementary Note 4**). The schematic diagram of detailed optical setup is shown in **Supplementary Note 3**). From the recorded data/images it is apparent that the photon emission from single molecule is random within the blinking period, and the corresponding PSFs have

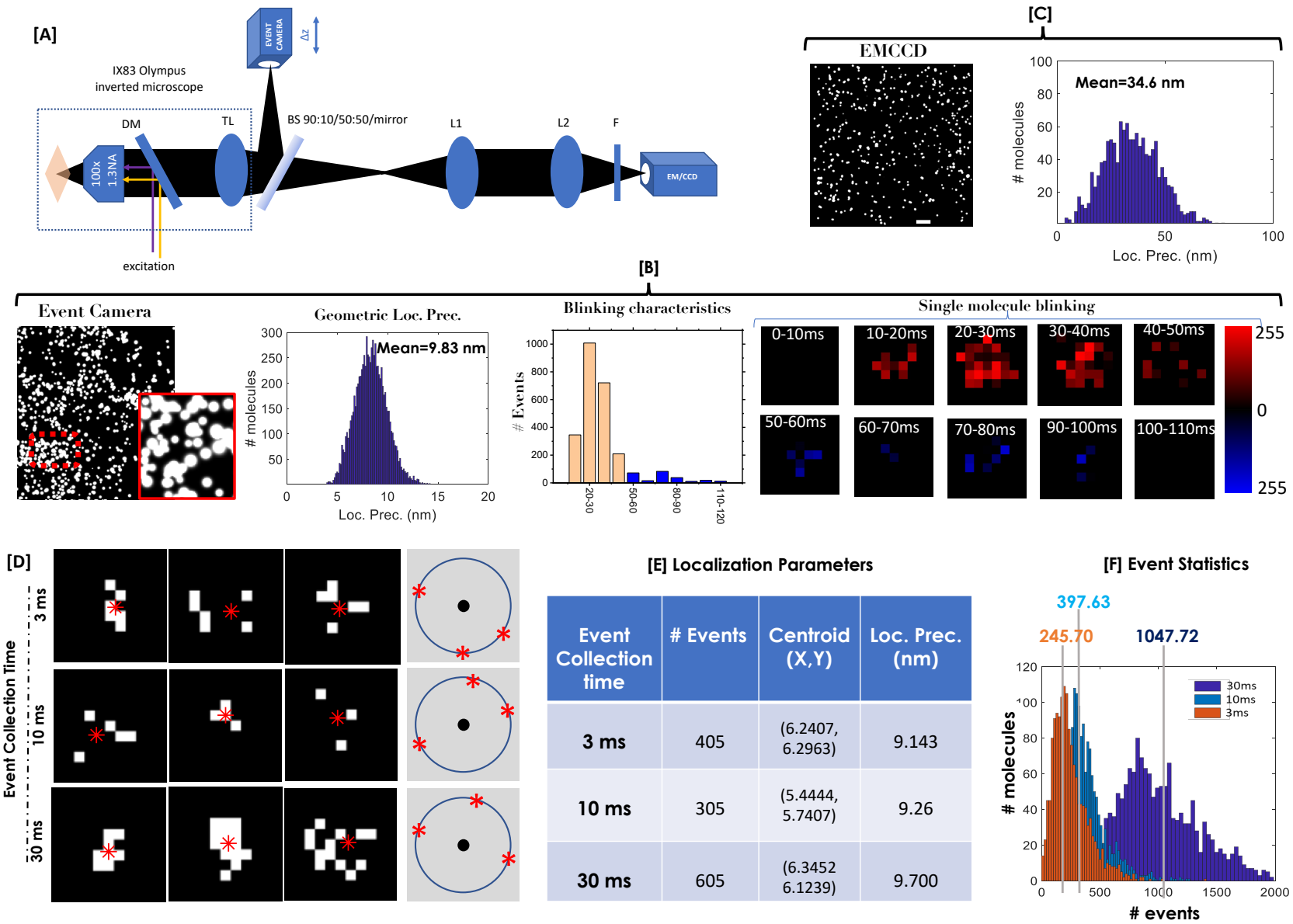

Event Collection time	# Events	Centroid (X,Y)	Loc. Prec. (nm)
3 ms	405	(6.2407, 6.2963)	9.143
10 ms	305	(5.4444, 5.7407)	9.26
30 ms	605	(6.3452 6.1239)	9.700

FIG. 2: [A] Schematic diagram of event camera integration in the detection subsystem of conventional SMLM. The complete system is shown in **Supplementary Note 3**. The detection arm is designed for simultaneous two-channel imaging. Event camera records images the reflected signal from the beam splitter (BS), whereas EMCCD records transmitted light/signal. The mirror is used to image 100% signal with an event camera only. [B] Event(both positive and negative) based reconstruction and geometric localization of reconstruction of cy3 molecules. Corresponding localization precision of mean 9.83nm along with positive and negative event distribution for frames collected over 10ms time. [C] EMCCD reconstructed recorded super resolved image using frame-based SMLM technique. Single molecules are localized at 34.6nm. [D] Event based segmented PSF(both positive and negative events) with centroid at collection time of 3ms,10ms and 30ms collection time. A circle is fitted through centroid of the segmented PSFs. Center and radius of the circles is used as position and localization precision of the molecule.[E] Geometric localization of PSF parameters. [F] Distribution of number of event detected(both positive and negative) in Cy3 molecules at varying collection time of 3ms, 10ms and 30ms.

distinct distributions. This is important from the point-of-view of super-resolution imaging, since this allows the localization of single molecules purely based on geometric parameters estimated from the recorded PSF (photon distribution). Alongside the reconstructed super-resolved image of Cy3 molecules (spread on a coverslip) is also shown. Localization of these molecules are calculated using geometric localization method (see, **Supplementary Note 4**). For comparison, reconstruction for standard SMLM (data acquired by EMCCD) along with localization precision (using Thompson's formula) is also shown in Fig. 2C [39]. Fig. 2D shows the distribution of a typical single molecule captured by event camera at a time sampling of 3 ms, 10 ms and 30 ms. Since the molecule blinking period is much longer, the event camera captures multiple realizations of bright PSF spots (with a large number of events) of a blinking molecule. Subsequently, the centroid of spot is determined from consecutive frames (see, red star in Fig. 2D). Assuming symmetric localization precision a circle is fit to the centroids (see, black dot in Fig. 2D). The centre and diameter of the circle is determined (see, Fig. 2D). This gives the position and localization precision for the single molecule. The corresponding localization parameters for a typical single molecule is tabulated in Fig. 2E, and detected event statistics at varying collection times of event detector is shown in Fig. 2F. Within the event collection time, the same process is repeated for all the molecules and a super-resolved map is constructed. The details of calculation for geometric localization precision is discussed in **Supplementary Note 4**. The localization precision plots indicate an average localization of 9.143 nm for $\tau = 3$ ms of a typical single molecule. This is about 3.5 times less than the localization precision of standard SMLM that use well-known Thompson's formula [39]. Overall, this suggests a spatio-temporal resolution of $l_p \times \tau = 9.143 \times 3$ $nm.msec$. This is way better than standard SMLM.

To substantiate the new technique, we imaged mitochondrial membrane protein (Tom20) labelled with mEos photoactivable probe. Fig. 3A shows the epifluorescence image of the mEos-Tom20 transfected image of which a small portion is chosen for study. The corresponding event based super-resolved image is shown in Fig. 3B. The standard SMLM image (reconstructed from the data/images captured by EMCCD camera) is also displayed for comparison. Two sub-regions (R1 and R2) are chosen and compared as shown in Fig. 3(B,C). The corresponding localization plot gives an average localization precision of 11.65 nm. This is way below the localization precision of standard SMLM which is 40.03 nm. Note that the data is obtained at $\tau = 30$ ms. Super-resolved images at other event

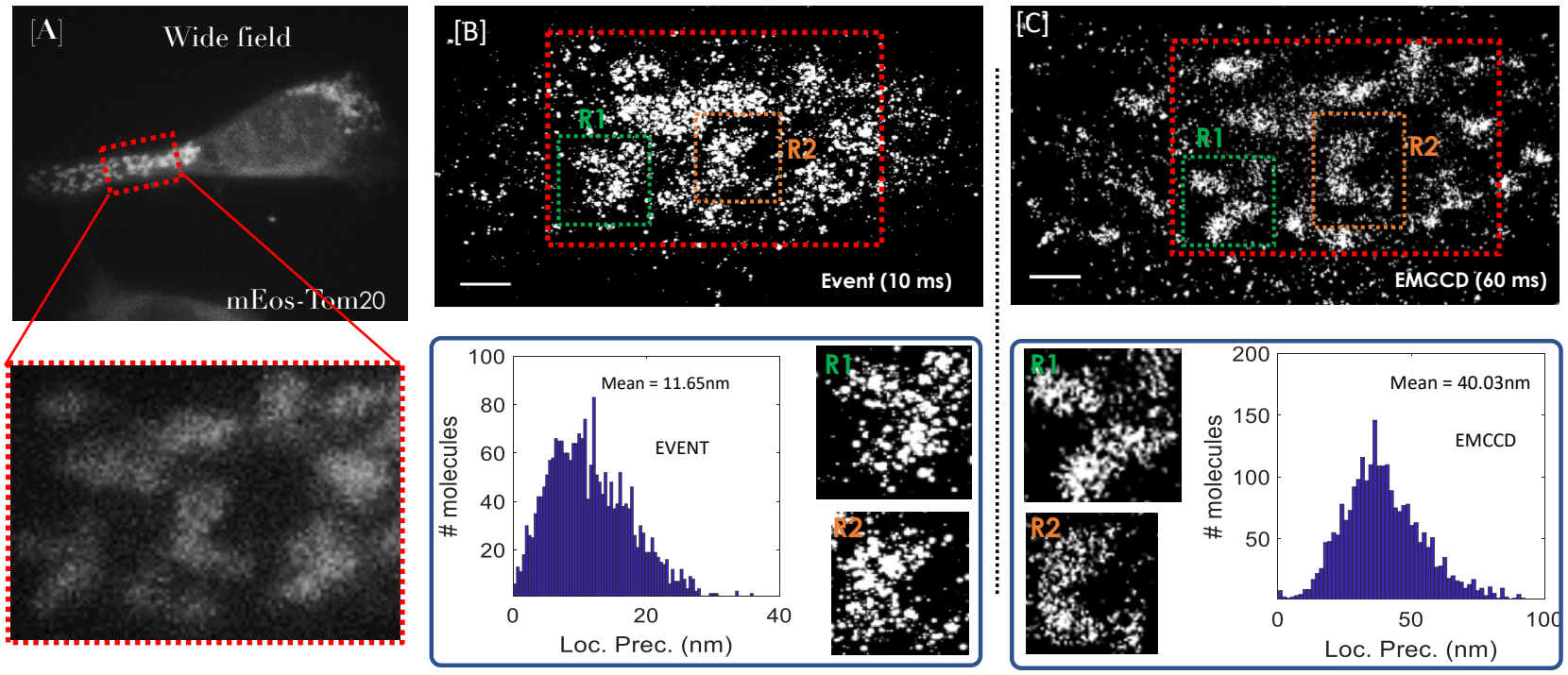

FIG. 3: [A] Widefield fluorescence image of mEosTom20 transfected fixed NIH3T3 cell. Red doted zone is ROI. [B] Event detection based reconstructed superresolved image of Tom20 molecules. Frames are constructed by collecting events over 10ms. In the frames each pixel gray levels equal to the sum of negative and positive events detected in 10ms. [C] Localization map of Tom20 molecules detected using EMCCD (30ms exposure time). Enlarge views show of regions R1 and R2 from [B] and [C] along with respective localization precision histogram. Data presented is simultaneous imaging using event and EMCCD camera.

collection times ($10 - 100\ ms$) is shown in **Supplementary Note 5**.

Next, we employ the proposed $eventSMLM$ system to understand spatio-temporal dynamics of HA molecules and its collective dynamics in an Influenza (type-A) disease model. Healthy NIH3T3 cells were transfected with a viral plasmid DNA (Dendra2-HA). This is followed by incubation at a temperature of 37^oC and 5% supply of CO_2. One set of cells were fixed by standard protocol (see, Methods section, IV.G) and the other set is washed with PBS and prepared for live imaging. Fig. 4A shows widefield fluorescence image of a fixed cell. The corresponding reconstruction using event camera is shown in Fig. 4B along with SMLM reconstructed image. Note that, SMLM super-resolved image is reconstructed using EMCCD camera. Specifically, two regions (R1 and R2) were chosen for detailed study as displayed in Fig. 4(B,C). Event based super-resolved images of HA clusters at varying event collection time ($10 - 100\ ms$) is shown in **Supplementary Note 6**. Alongside, the localization precision is also shown which indicate an average localization precision of 12.25 nm. Since the frame is captured in 10 ms as compared to 60 ms (30 ms for capture + 30 ms for read/write) for SMLM, this shows a 6 times improvement in temporal resolution. Overall the system shows an impressive spatio-temporal resolution ($l_p \times t$) of $\sim 12.25 \times 10\ nm.\ msec = 12.25 \times 10\ p$, where, $1p = 10^{-12}\ meter.second$. This is approximately, 14.69 times better than SMLM for which standard spatio-temporal resolution is, $\sim 30 \times 60\ p$. The corresponding FRC analysis for both the samples (mEos-Tom20 and Dendra2-HA) is discussed in **Supplementary Note 7**.

To further validate the event-based single molecule super-resolution microscopy ($eventSMLM$), we have used it to visualize HA single molecules in Dendra2-HA transfected NIH3T3 cells (The cells are fixed post 24 hrs of transfection). The reconstructed super-resolved image of HA distribution for varying event collection time is shown in Fig. 5A. Alongside overlay of all the images is shown that indicate more HA molecules per cluster for 100 ms, thereby completing individual clusters. In addition, a comparison of event based detection (data acquired using event camera) and frame based detection (EMCCD camera used for SMLM) is shown in Fig. 5B. Note that, simultaneous data acquisition is achieved for both the camera using 90 : 10 beam-splitter (90 for event camera and 10 for EMCCD) for comparison. Alongside an overlay of both the data suggests high-level colocalization of 0.8156. In addition, we have estimated biophysical parameters independently for both the detection schemes (event and frame) as shown in Table S8-T (see, **Supplementary Note 8**). A strong overlap of clusters indicate reliability of event-based super-resolution microscopy (see, Fig. 5B). This strengthens the fact that, event-based detection has high degree of dependability along with the added advantage of high spatio-temporal resolution.

To access the potential of $eventSMLM$ system, we have used it to visualize HA dynamics in live cells. The system is configured to take time-lapse data / images at a rate of 10 ms after every 15 minutes. Note that, event camera take continuous data with a negligible registration time of 100 μsec, whereas EMCCD camera needs about 30 $msec$ for data registration after collecting data for each frame. For the live experiment, the data is collected continuously over 60 minutes by the event detector, and the same is shown in Fig. 6A. Prominent clusters are identified using DBSCAN algorithm [41] and the individual clusters are colored (see, Fig. 6A). In addition, a separate binary cluster map considering only the clustered molecules is shown in Fig. 6B. Alongside, the overlay of all the images are also displayed. This clearly indicates dynamic evolution, formation and even migration of HA clusters in the transfected live cell. The corresponding plot indicates near equal value of localization precision for data taken over 60 minutes suggesting the bias-free data acquisition without significant photo-bleaching effect (see, Fig. 6C). We have also estimated biophysical parameters at every time-point as shown in Fig. 6(D,E). This indicates equal density of HA clusters and an increasing cluster fraction that suggests active HA participating in cluster formation post 24 hrs of transfection. More details related to HA cluster dynamics is discussed in **Supplementary Note 9**.

The experiments on fixed and live cells clearly indicate the advantage of event-based detection over frame-based detection employed in existing SMLM techniques. With the further development of event-based detection, single molecule imaging techniques are likely to play key roles in terms of high spatio-temporal super-resolution and low-cost of ownership.

III. DISCUSSION

Single-molecule super-resolution microscopy is taking biology by storm, revealing events that were once thought impossible. Several

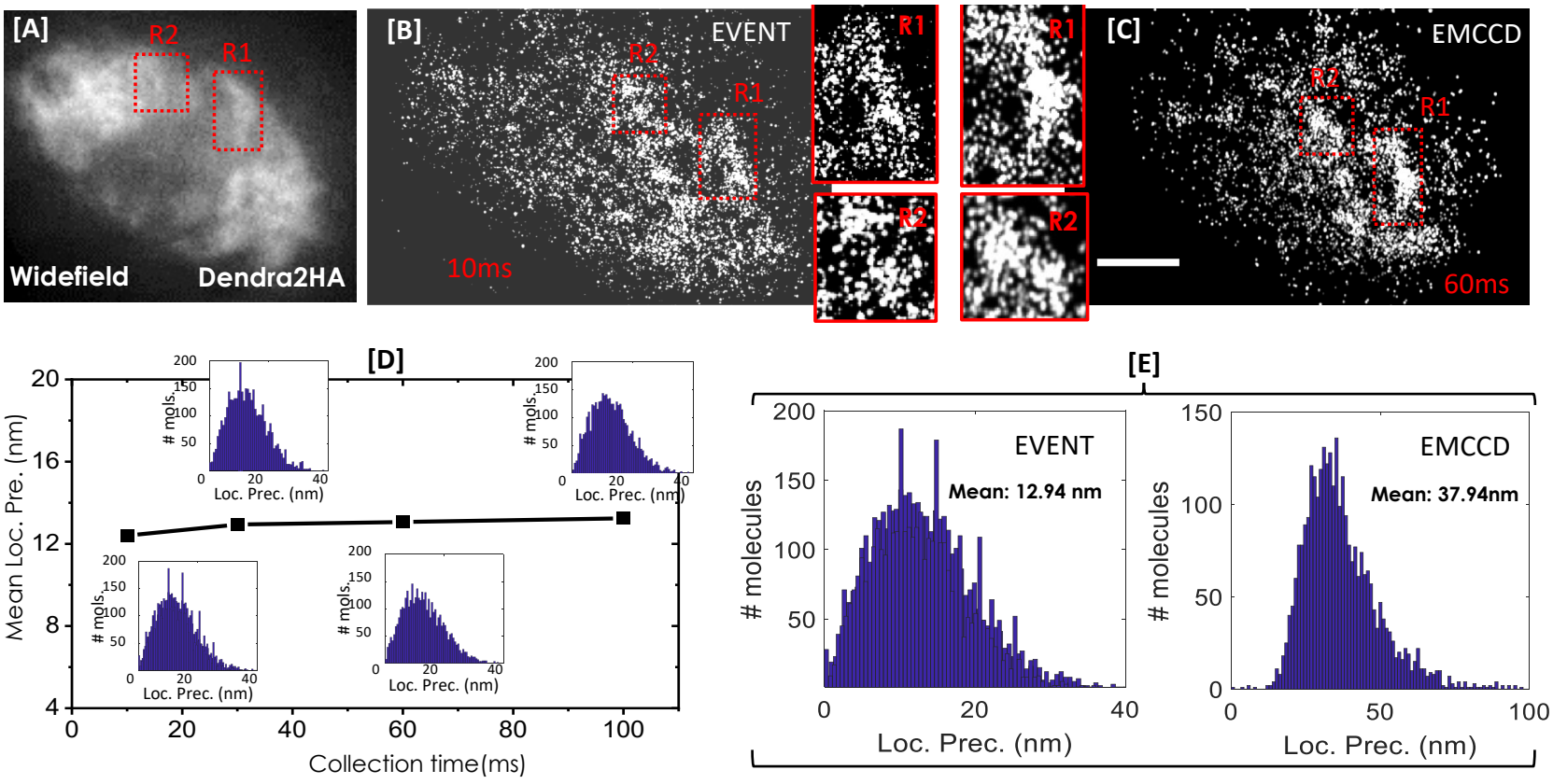

FIG. 4: [A] Widefield fluorescence image of Dendra2HA transfected fixed NIH3T3 cell. [B] Event based reconstructed superresolved image. Frames are constructed by collecting all the events over 10ms. [C] Super-resolved map (SMLM) of HA molecules recorded by EMCCD (30ms exposure time). Enlarge view of ROIs (R1 and R2) also shown. [D] Event based Localization precision variation with event collection time. [E] Localization precision of the molecules detected by event detector(left) and EMCCD (right). Data presented is simultaneously detected by event and EMCCD. Scale bar= $1\mu m$.

studies have been reported over the last decade that demonstrate the capability of SMLM to reveal biological processes with single-molecule precision. Much credit goes to the development of new detectors that have accelerated SMLM imaging [40]. However, existing SMLM has poor temporal resolution, and the need for spatial resolution beyond sub-10 nm has increased over time. In this respect, event-based super-resolution microscopy is likely to play a big role, which is predominantly due to its ability to detect events, thereby pushing the limits of spatio-temporal resolution, $< 1p$ (where $1p = 10^{-12}\ ms$).

The fact that the event camera is sensitive to changes in intensity gives it the additional capability to detect positive / negative changes. Unlike the existing SMLM that employ EMCCD/sCMOS detectors, event detector can continuously take data. This is incredible since no signal / photon is lost during the entire period of investigation. For the present study, $eventSMLM$ is first demonstrated by simply switching on/off the photon stream of a laser source and subsequently using Cy3 blinking (see Fig. 2). Interestingly, Cy3 imaging has revealed non-zero events (photon emission) within the blinking period comprising both positive and negative events. This exposes the characteristic nature of photon emission from a single molecule within the blinking period.

Since the event camera does not directly reveal the number of photons but rather gives the change in the number of photons, the use of Thomson's formula may not be appropriate [39]. To deal with this the localization precision is calculated geometrically as discussed in **Supplementary Note 4**. The method determines centroids from multiple realizations (PSF images)of single-molecule collected within the blinking period. From this set of centroids, a circle is fit, giving its center and radius. This center and radius of the circle are taken as the position and geometric localization precision, and the super-resolution map is reconstructed. Unlike Thompson's formula, geometric localization precision is purely data-driven. For example, a spatial resolution (measured in terms of localization precision) of $< 10\ nm$) along with a temporal resolution of $< 10\ msec$ produced an image with a spatio-temporal resolution of $< 100p$. This is a multi-fold improvement over the existing SMLM techniques. All together, event-based super-resolution microscopy brings a novel capability for investigating biological processes in both fixed and live cells.

The proposed microscopy technique is employed to visualize the arrangement of mitochondrial membrane protein (Tom20) labeled with mEos, on the mitochondrial membrane (see Fig. 3). The results revealed $\sim$ 4-fold improvement in localization precision, apart from high temporal resolution. In addition, the technique is used to investigate HA clusters in transfected NIH3T3 cells with an impressive localization precision of 12.94 nm and a 6-fold improvement in temporal resolution (see Fig. 4). Altogether, an improvement in spatio-temporal resolution of $\sim$ 14.69 is noted when compared to standard SMLM. The study over a range of collection time and its effect on the quality of the reconstructed image (with respect to HA clusters) indicate the robustness and consistency of the proposed microscopy technique (see Fig. 5). The technique ($eventSMLM$) further allowed determination of biophysical parameters (see, Fig. 6 and **Supplementary Note 8**). Finally, the technique was tested on live cells (post 24 hrs of transfection) to visualize the formation of HA clusters over a period of time. For the first time, we could visualize the formation of HA clusters using event-based single-molecule detection. This is in addition to the estimation of dynamic biophysical parameters (# clusters, $\#HA$/cluster, cluster density, and cluster-fraction) on the go (see, Fig. 6). Overall, the advantage of event-based SMLM is apparent considering the complexity of processes involved in cellular system.

Future developments are likely to see an increased use of event cameras for single-molecule imaging. Further developments of event cameras with better quantum efficiency are likely to improve the temporal resolution in micro/nano-second time scale, thereby further pushing the limit of spatio-temporal resolution to reveal biological processes in action.

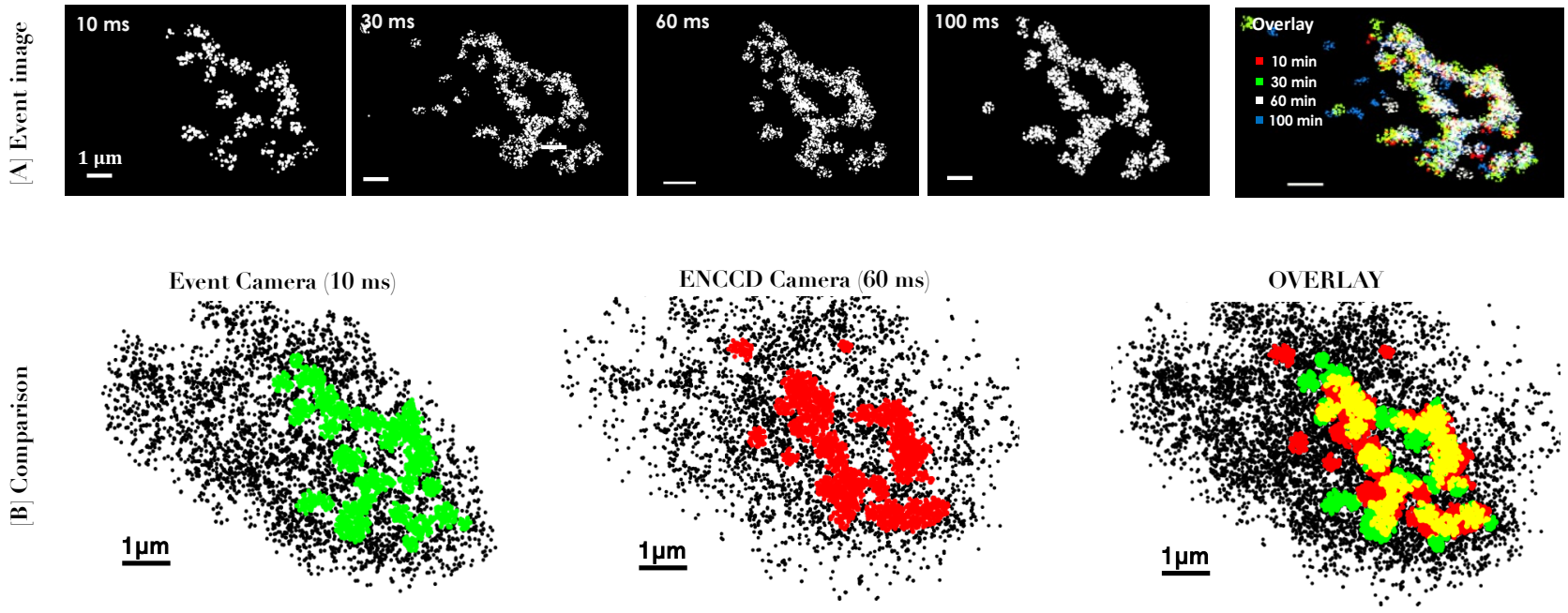

FIG. 5: [A] DBSCAN algorithm applied to identify the cluster of HA molecules in a fixed NIH3T3 cell at varying collection event time of 10ms, 30ms, 60 ms and 100ms. [B] Event detected HA cluster (10ms event collection time) is compared with EMCCD detected cluster. The cluster is found to be consistent(see overlay image) with colocalization factor of 0.8156.

IV. MATERIALS AND METHOD

A. Toggle ON/OFF event setup

To experimentally generate ON/OFF events, we build an optical system, as shown in the Fig. 1. Complete details of each component can be found in **Supplementary Note 2**. A continuous beam of $532nm$ approximately $1mm$ beam diameter is expanded $4X$ times by using a beam-expander system that comprises of two biconvex lenses of focal lengths, $2.5mm$ and $10mm$. The expanded beam is spit into two paths using a beam splitter 50 : 50. Each split beam is focused on the detector by Olympus $10X, 0.3NA$ objective lens. One of the focused spots is projected on the event camera, and the other spot is projected in a frame-based camera (CCD/EMCCD). To toggle the 532nm continuous laser ON/OFF, we used an electronics chopper in the path of the beam. The toggling ON/OFF and camera capture is synchronized using a microcontroller (Arduino). Toggle ON/OFF time can be set in the script code.

B. Optical setup of $eventSMLM$

The key optical component of the $eventSMLM$ system along with other details can be found in **Supplementary Note 3**. Light beams from activation excitation lasers of wavelengths, 405 nm and 561nm are combined by a dichroic mirror, and the combined beam is coupled with IX81 Olympus inverted microscope (used in epifluorescence mode). Illumination and collection of the fluorescence were done with oil immersion Olympus 100x 1.3NA. The dichroic filter instated in the microscope helps to distinguish excitation and emission wavelengths. Distinguished fluorescence is directed to the detection subsystem that is capable of imaging two channels to facilitate simultaneous capture of the signal using an event camera and EMCCD. We used beam splitter to simultaneous capture signals in both the detectors. In the EMCCD detection path, an additional magnification of 2X is introduced to satisfy the sampling criteria. A set of optical filters are used in the detection path to collect fluorescence signal. The present configuration results in an effective pixel size of 45nm and 85nm for the event camera and EMCCD, respectively.

C. Data acquisition

The data acquisition begins with identifying transfected cells using a separate fluorescence arm (not shown). Subsequently, the cell is prepared for super-resolution imaging. For quality imaging, the lasers are optimized for stable blinking of the molecules by matching the intensities that control the activation and emission rates [3]. A laser power of 20mW and $6\mu W$ for 560nm and 405nm is used. All data presented in this manuscript is acquired simultaneously in both the detectors. In EMCCD, the data are acquired in a stack of .tif format with 30ms exposure. Event camera parameters are optimized and key imaging parameters such as, field of view(FOV), sensitivity, and polarity sensitivity are set for data collection.

D. Event based frame generation

Any pixel of the event camera records a stream of events (x, y, t, p) where, (x, y) is pixel coordinate, t is the time at which intensity change occurs, and p is the polarity of events. Positive polarity corresponds to positive change in intensity; the corresponding event is called positive event, whereas negative polarity corresponds to a negative change in intensity, and the corresponding event is called negative event. One can reconstruct frames from any event type, i.e, positive event frames, negative events only frames or including both positive and negative events frame. Images of 8-bit .tif format of 10ms,30ms,60ms and 100ms time binned events (both positive and negative) are generated. The code for generating from events is written in phyton script. Details on different event frame construction algorithms can be found in Ref. [42]. Details on working of event camera can ve found in **Supplementary Note 1**.

E. Event based image reconstruction

A customizable Matlab script is written to reconstruct the super-resolved image. Approach similar to conventional super-resolved image reconstruction are applied. Initially, event-based particle identification is carried out. This step includes morphological operation with suitable structuring elements. This pre-processing step helps in reducing unwanted signals. The left-out particle-like spots are identified using a correlation approach. An ideal PSF is correlated with the pre-processed image, and based on the threshold correlation value, particles are identified. Only the particles which are repeating in subsequent frames (atleast 3 frames) or more are considered to be molecules (within the blinking period of a molecule). A circle is fit through the centroids for which centre and radius is determined. The centre and diameter of the blinking molecule is taken as the position and localization precision. We presented the intensity of the molecules proportional to the sum of events in each frame. Accordingly, we have the estimated molecule information centroid, localization precision, and intensity. Hence in the super-resolved image, each molecule

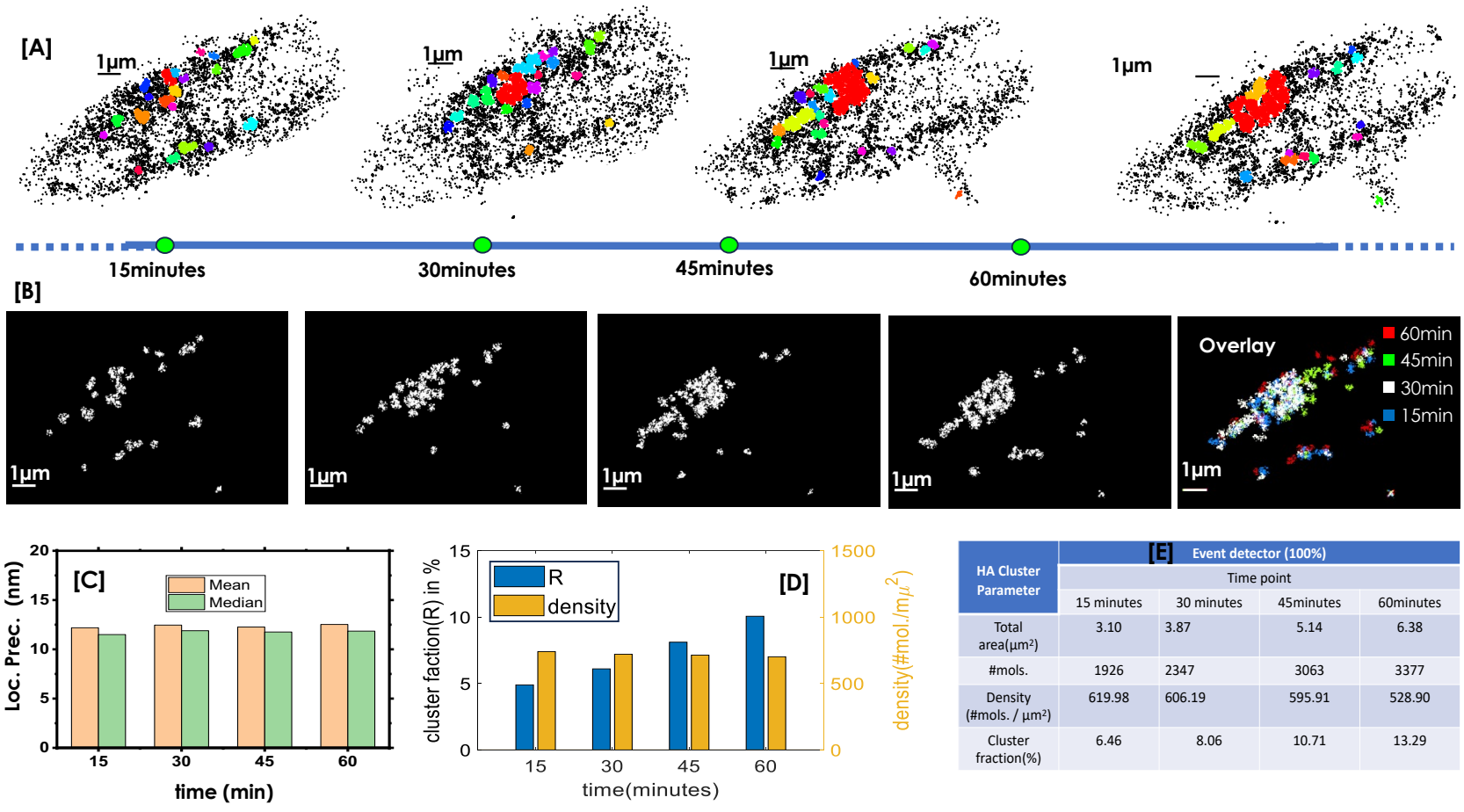

HA Cluster Parameter	[E] Event detector (100%)			
	Time point			
	15 minutes	30 minutes	45minutes	60minutes
Total area(µm²)	3.10	3.87	5.14	6.38
#mols.	1926	2347	3063	3377
Density (#mols. / µm²)	619.98	606.19	595.91	528.90
Cluster fraction(%)	6.46	8.06	10.71	13.29

FIG. 6: **Live Cell Imaging:** [A] DBSCAN algorithm applied to identified the dynamics of HA clusters in *eventSMLM* super-resolve images. Frames were reconstructed using 10 ms event collection time. [B] Map of only clustered HA molecules (unclustered molecules are removed). Color coded time overlay are also shown. [C] Variation of localization precision with time. [D] Change in cluster fraction (percentage of clustered molecules) and density of the HA molecules in clusters with time. [E] Tabulated biophysical parameters related to HA clusters. Mirror is used to detect 100% signal / fluorescence.

detected is represented with a Gaussian centered at the centroid, and the spot size equals localization precision. More details can be found in **Supplementary Note 4**.

F. Fluorescent proteins

To begin with the event-based detection of single molecules, we used the well-known fusion fluorescence protein mEosTom20. The plasmid is frequently used to visualize the Tom20 protein molecules, which are located at the mitochondrial outer membrane. The plasmid were purchased from Addgene, USA. The non-activated mEOSTOM20 can be visualized at 532nm upon blue 488nm excitation. After absorption of 405nm light, the absorption peak of molecules shift to 563nm and emission peak to 573nm.

Another fusion plasmid, Dendra2HA, is used to visualize the HA molecules in the plasma membrane of the cell after 24 hours post-transfection. HA is an influenza-type A viral protein. Event-based detection of HA molecules in fixed and live cells is demonstrated post-transient transfection.

G. Cell culture and transfection:

The study used mouse fibroblast NIH3T3 cell lines. 3T3 cells preserved in LN2 was thawn and cultured using standard protocols. After two passages, the cells were seeded with a count of approximately 10^5 and cultured in a 35mm disc with coverslip for transfection. Post 24hr, the cells were used for transfection. Lipo P3000 transfection protocol is used to transfect cell with both the plasmids dendra2HA and mEOSTOM20. The concentration of plasmid used are 1078 $ng/\mu l$ and 967 $ng/\mu l$ for dendra2HA and mEosTom2O. After 24hr, cells were washed with PBS 3X before fixing with 1% paraformaldehyde. Fixed cells are mounted with fluor save and air tighten by nail paint. For live imaging of 3T3 cells same transfection protocol is adopted and imaging is done in growth median after 24hrs post transfection.

SUPPLEMENTARY MATERIAL

Supplementary Note 1. Event camera: working principle and calibration.

Supplementary Note 2. Toggle ON/OFF Event detection with event camera.

Supplementary Note 3. Complete optical setup of the *eventSMLM* system.

Supplementary Note 4. Event based geometric localization of single molecules and image reconstruction.

Supplementary Note 5. Super-resolving mitochondrial network (mEos-Tom20) in cellular system.

Supplementary Note 6. Event based super-resolution imaging of Dendra2-HA clusters in transfected cell.

Supplementary Note 7. FRC analysis for eventSMLM reconstructed images.

Supplementary Note 8. Estimation of critical biophysical parameters.

Supplementary Note 9. Event based imaging of cluster dynamics in a live cell.

Competing Interests: The authors declare no competing interests.

Contributions: PPM and JB conceived the idea. JB, AS, NP and PPM prepared the samples, and carried out the experiments. JB, AS, NP, VR, CST, PPM analyzed the data and prepared the figures. PPM wrote the paper by taking inputs from all the authors.

[1] T. A. Klar, and S. W. Hell, “Subdiffraction resolution in far-field fluorescence microscopy”, Opt. Lett. 24, 954(1999).

[2] M. J. Rust, M. Bates and X. Zhuang, “Sub-diffraction-limit imaging by stochastic optical reconstruction microscopy (STORM)”, Nat. Methods, 3, 793 (2006).

[3] S. T. Hess, T. P. Girirajan and M. D. Mason, “Ultra-high resolution imaging by fluorescence photoactivation localization microscopy”, Biophys. J., 91, 4258(2006).

[4] E. Betzig , George H Patterson, Rachid Sougrat, et al, “Imaging intracellular fluorescent proteins at nanometer resolution”, Science, 313, 1642(2006).

[5] Sharonov, A. and Hochstrasser, R.M., “Wide-field subdiffraction imaging by accumulated binding of diffusing probes”, Proc. Natl. Acad. Sci. USA 103, 18911(2006).

[6] Lelek, M., Gyparaki, M.T., Beliu, G. et al., “Single-molecule localization microscopy”, Nat Rev Methods Primers 1, 39 (2021).

[7] Hell, S. W., Wichmann, J.,”Breaking the diffraction resolution limit by stimulated emission: Stimulated-emission-depletion fluorescence microscopy”. Optics Letters. 19, 780(1994)

[8] Stefan W Hell, “Far-field optical nanoscopy”, Science 316, 1153 (2007).

[9] Mats G. L. Gustafsson, ‘Nonlinear structured-illumination microscopy: Wide-field fluorescence imaging with theoretically unlimited resolution”, PNAS (USA) 102 13081(2005).

[10] F. Balzarotti, Y. Eilers, K. C. Gwosch, A. H. Gynnå, et al, “Nanometer resolution imaging and tracking of fluorescent molecules with minimal photon fluxes,” Science, 355, 606(2016).

[11] Reinhardt, S.C.M., Masullo, L.A., Baudrexel, I. et al., “Ångström-resolution fluorescence microscopy”, Nature, 617, 711(2023).

[12] Yu Lin,Jane J. Long,Fang Huang,Whitney C. Duim et al., “Quantifying and Optimizing Single-Molecule Switching Nanoscopy at High Speeds”, Plos One , 10,e0128135 (2015).

[13] C. Laplante, F. Huang, J. Bewersdorf, T. D. Pollard , “High-Speed Super-Resolution Imaging of Live Fission Yeast Cells”, Methods in Molecular Biology 1369,45(2016).

[14] Diekmann, R., Kahnwald, M., Schoenit, A. et al , “Optimizing imaging speed and excitation intensity for single-molecule localizationmicroscopy”, Nat. Meth. 17, 909(2020).

[15] Zhen-Li Huang, Hongyu Zhu, Fan Long, Hongqiang Ma, et al., “Localization-based super-resolution microscopy with an sCMOS camera”, Opt. Exp. 19, 19156(2011).

[16] Huang, B., Wang, W., Bates, M. & Zhuang, X. “Three-dimensional super-resolution imaging by stochastic optical reconstruction microscopy”, Science 319, 810(2008).

[17] Manuel F Juette, Travis J Gould, Mark D Lessard, Michael J Mlodzianoski, et al. “Three-dimensional sub-100 nm resolution fluorescence microscopy of thick samples”, Nat. Methods 5, 527 (2008).

[18] Sri Rama Prasanna Pavani, Michael A. Thompson, Julie S. Biteen et al. “Three-dimensional, single-molecule fluorescence imaging beyond the diffraction limit by using a double-helix point spread function”, Proc. Natl Acad. Sci. USA 106, 2995(2009).

[19] Dasgupta, A., Deschamps, J., Matti, U. et al. Direct supercritical angle localization microscopy for nanometer 3D superresolution. Nat Commun, 12, 1180 (2021).

[20] Lelek, M., Di Nunzio, F., Henriques, R., Charneau, et al, “ Superresolution imaging of HIV in infected cells with flash palm”, Proc. Natl. Acad. Sci. U S A 109, 8564(2012).

[21] Szymborska, A., De Marco, A., Daigle, N., Cordes, V.C., et. Al, “Nuclear pore scaffold structure analyzed by super-resolution microscopy and particle averaging”, Science, 341, 655(2013).

[22] Salvador-Gallego, R., Mund, M., Cosentino, K., Schneider, J., et al, “Bax assembly into rings and arcs in apoptotic mitochondria is linked to membrane pores”, EMBO J. 35, 389(2016).

[23] C. A. Valades Cruz, H. A. Shaban, A. Kress, N. Bertaux, S. Monneret, M. Mavrakis, J. Savatier, and S. Brasselet, “Quantitative nanoscale imaging of orientational order in biological filaments by polarized superresolution microscopy,” Proceedings of the National Academy of Sciences, 113, E820(2016).

[24] Nahidiazar L, Agronskaia AV, Broertjes J, van den Broek B, Jalink K,” Optimizing Imaging Conditions for Demanding Multi-Color Super Resolution Localization Microscopy”, PLoS ONE, 11, e0158884(2016)

[25] Xinghua Shi, John Lim, and Taekjip Ha,” Acidification of the oxygen scavenging system in single-molecule fluorescence studies: in situ sensing with a ratiometric dual-emission probe” ,Analytical Chemistry, 82, 6132(2010)

[26] A. Kinkhabwala, Z. Yu, S. Fan, Y. Avlasevich, K. Müllen, and W. E. Moerner, “Large single- molecule fluorescence enhancements produced by a bowtie nanoantenna,” Nature Photonics, 3, 654(2009).

[27] D. Bouchet, J. Scholler, G. Blanquer, Y. D. Wilde, I. Izeddin, and V. Krachmalnicoff, “Probing near-field light–matter interactions with single-molecule lifetime imaging,” Optica, 6, 135(2019).

[28] M. P. Backlund, M. D. Lew, A. S. Backer, S. J. Sahl, and W. E. Moerner, “The role of molecular dipole orientation in single-molecule fluorescence microscopy and implications for super-resolution imaging,” ChemPhysChem, 15, 587(2014).

[29] Yang Zhang, Ki-Hee Song, Biqin Dong, Janel L. Davis, Guangbin Shao, Cheng Sun, and Hao F. Zhang, ”Multicolor super-resolution imaging using spectroscopic single-molecule localization microscopy with optimal spectral dispersion” Appl Opt., 58, 2248 (2019).

[30] Mlodzianoski MJ, Curthoys NM, Gunewardene MS, Carter S, Hess ST, “ Super-Resolution Imaging of Molecular Emission Spectra and Single Molecule Spectral Fluctuations”, PLoS ONE 11(3): e0147506(2016).

[31] Yunjae Suh, Seungnam Choi, Masamichi Ito, Jeongseok Kim et al., ” A 1280x960 dynamic vision sensor with a 4.95- mu pixel pitch and motion artifact minimization ”, Proc. IEEE Int. Symp. Circuits Syst., 1(2020).

[32] Guillermo Gallego, Tobi Delbrück, Garrick Orchard, Chiara Bartolozz et al., ”Event-Based Vision: A Survey”, IEEE Transactions on Pattern Analysis and Machine Intelligence, 44, 154(2022).

[33] A. Lakshmi, A. Chakraborty, C. S. Thakur, “Neuromorphic vision: From sensors to event-based algorithms”, Wires 9, e1310 (2019).

[34] Mangalwedhekar, R., Singh, N., Thakur, C.S. et al., “ Achieving nanoscale precision using neuromorphic localization microscopy”, Nature Nanotech. 18, 380(2023).

[35] Xiaohui Qu, David Wu, Laurens Mets, and Norbert F. Scherer Nanometer-localized multiple single-molecule fluorescence microscopy, Proc Natl Acad Sci U S A, 101, 11298(2004).

[36] T. Ha, Th. Enderle, D.S. Chemla, P.R. Selvin , and S. Weiss , “Quantum jumps of single molecules at room temperature”, Chemical Physics Letters, 271, 1(1997).

[37] Shtengel, G., Hess, H. F., Lippincott-Schwartz, J. & Manley, S. , “Interferometric fluorescent super-resolution microscopy resolves 3D cellular ultrastructure”, Proc. Natl. Acad. Sci. USA 106, 3125(2009).

[38] Christian Steinhauer, Carsten Forthmann, Jan Vogelsang, and Philip Tinnefeld, “ Superresolution Microscopy on the Basis of Engineered Dark States”, J. Am. Chem. Soc.130, 16840(2008).

[39] R. E. Thompson, D. R. Larson, W. W. Webb, “Precise Nanometer Localization Analysis for Individual Fluorescent Probes”, Biophys. J., 82, 2775(2002).

[40] Jigmi Basumatary, Neptune Baro, Fancesca Cella Zanacchi and Partha Pratim Mondal, “Temporally resolved SMLM (with large PAR shift) enabled visualization of dynamic HA cluster formation and migration in a live cell”, Sci. Rep. 13, 12561 (2023).

[41] Jigmi Basumatary, Neptune Baro, Prakash Joshi and Partha Pratim Mondal, “Scanning single molecule localization microscopy (scanSMLM) for super-resolution volume imaging” , Comm. Biol., 1050 (2023).

[42] L. Annamalai, V. Ramanathan, C. S. Thakur, “Event-LSTM: An Unsupervised and Asynchronous Learning-Based Representation for Event-Based Data”, IEEE Robot. Auto., 7, 4678 (2022).